



# INTERACTION MECHANISM BETWEEN GEOCELL REINFORCEMENT AND GRAVELLY SOIL BY PULLOUT TESTS

Xinye HAN<sup>1</sup>, Takashi KIYOTA<sup>2</sup> and Fumio TATSUOKA<sup>3</sup>

**ABSTRACT:** To increase the pullout resistance of geocell, a square-shaped geocell was developed and pullout tests were conducted on small scaled models placed in gravelly soil backfill. A preloading method was applied to enhance a high initial stiffness of square-type geocell. Significant effects of in-plane geometry and height of geocell on the pullout resistance were found. Analysis of the test results indicates noticeable particle size effects that can be explained by a conceptualized pullout interaction mechanism. It is shown that the pull-out resistance is composed of two factors: the shear resistance along the shear bands developed at the top and bottom interfaces between the geocell and the adjacent backfill and the anchorage resistance induced by passive pressure inside the aperture of the geocell, which increases and becomes more dominant in the total pull-out resistance with an increase in the height of geocell.

**Key Words:** geocell, particle size effect, interaction mechanism, pullout resistance

## INTRODUCTION

Geosynthetic-reinforced soil structures are now widely used for different civil engineering applications, including earth retaining walls, bridge abutments, slopes, embankments, pavements and erosion control. Geocell, as a three-dimensional soil confinement system, has more attractive features than other planar geosynthetic reinforcements such as geotextiles and geogrids (Yuu and Han, 2008).

Most of the previous studies of geocell were mainly focused on the function as base reinforcements subjected to vertical loads, such as roads, embankments, light houses. The influencing factors for the performance of geocell-reinforced bases, such as geometric structures and dimensions, properties of geocell material and properties of infilled soil, loading methods, etc., were investigated by many researchers including Rea and Mitchell (1978), Shimizu and Inui (1990), Mhaiskar and Mandal (1992b, 1994), Dash et al. (2001a, 2001b, 2003, 2004), etc.

For the last two decades, geosynthetic-reinforced soil retaining walls (GRS RWs) with a stage-constructed full-height rigid (FHR) facing have been constructed for railways, highways and other facilities and have shown greater seismic resistance than conventional retaining wall structures (Tatsuoka et al., 2009). Geogrids and geotextiles are commonly used as planar reinforcements to tensile-reinforce the backfill of RWs, embankments and other soil structures. However, the application of geocell as tensile reinforcement to these soil structures is relatively new due to the lack of related research. Ling et al. (2009) investigated the seismic performance of several soil RWs having a geocell facing by shaking table tests. The results showed that walls having a geocells facing are flexible exhibiting much better seismic performance than conventional type RWs. In addition, the performance

---

<sup>1</sup> Ph. D. student, Institute of Industrial Science, University of Tokyo

<sup>2</sup> Associate professor, Institute of Industrial Science, University of Tokyo

<sup>3</sup> Professor, Department of Civil Engineering, Tokyo University of Science

of a RW with the backfill reinforced with geocell layers was better than a RW with the backfill reinforced by geogrid layers.

One of the important advantages of geocell is an ability of three-dimensionally confining large particles in the cells exhibiting a large anchorage capacity when pulled laterally. Kiyota (2009) and Kuroda (2012) conducted a series of pullout tests using diamond-shaped geocell models and several different types of geogrids to investigate whether or not the geocells can be used as tension reinforcement. It was found that, although the diamond-type geocell shows higher pullout resistance than geogrids, the global stiffness is not better than the geogrids due to progressive large deformation of diamond-shaped cells. In the present study, in order to increase the initial stiffness and pullout resistance of geocell, a new type geocell having square cells were developed and evaluated by pull-out tests.

## TEST APPARATUS, PROCEDURES AND MATERIALS

### *Pullout test apparatus*

Figure 1 shows the schematic diagram of pullout test apparatus that was developed at IIS, the University of Tokyo. The tests were carried out on plane-strain condition. The pullout test apparatus is rectangular in shape and made of steel. The dimensions of inner soil box are 700mm (length)  $\times$  400mm (width)  $\times$  500mm (height). The opening size of the front wall can be changed for pulling out the model geocells of different heights. Papers are provided at the opening of the front wall to prevent the soils falling out during pullout tests. Leads shots are applied on the crest of the backfill to provide a surcharge of 1 kPa and a flexible top boundary, which is preferred for the purpose of measuring dilatancy of soil.

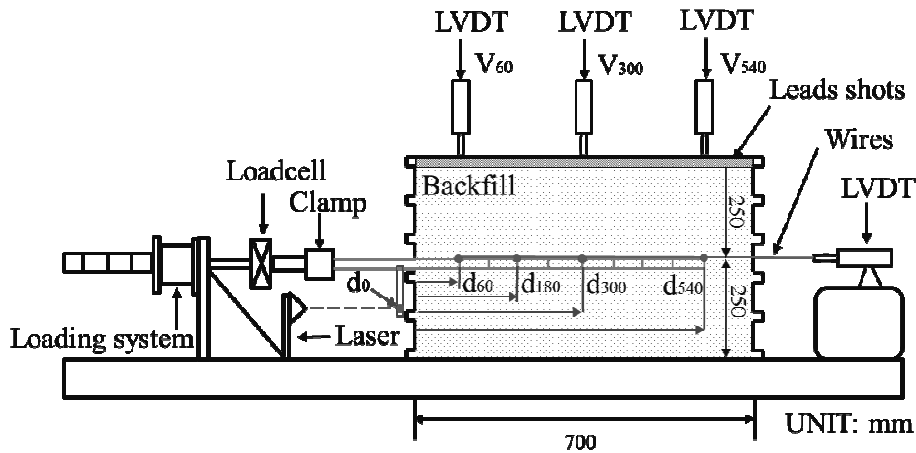


Figure 1. Schematic diagram of pullout test apparatus

### *Pullout test procedures*

Gravels were poured into the soil box and compacted in 25 cm-thick sub-layers arranging geocell model at the prescribed level in the backfill. The target density of the backfill was  $1.76\text{g/cm}^3$ . As listed in Table 1 and indicated in Figure 1, the front displacement ( $d_0$ ) was monitored by laser. The displacements along the geocell, for example, the locations at distances of 60 mm ( $d_{60}$ ), 180 mm ( $d_{180}$ ), 300 mm ( $d_{300}$ ), and 540 mm ( $d_{540}$ ) from the face of front wall were measured with Linear Variable Displacement Transducer (LVDTs). Monitoring the displacements along the geocell reinforcement allows proper interpretation of the interface load transfer mechanism and provides appropriate evaluation of the pullout resistance as well. Inextensible stainless wires were connected to the

designated locations of geocell reinforcement to measure the displacements along the geocell reinforcement. The wires were protected by stiff tubes and connected to the LVDTs, which were mounted on the rear wall of soil box. In addition, the vertical displacements at distances of 60 mm ( $V_{60}$ ), 300 mm ( $V_{300}$ ), and 540 mm ( $V_{540}$ ) from the face of the front wall were also measured with three LVDTs. The tests were conducted by pulling out the geocell at a constant displacement rate of 5 mm/min using a precision jack driven by a motor. The pullout force was measured with a load cell. All instrumentations were linked to an electronic datalogger which can scan the measurements at desired time intervals.

**Table 1.** Physical quantities measured in the tests

Measured physical quantities	Symbols
Displacement near wall	$d_0$
Horizontal displacements	$d_{60}, d_{180}, d_{300}, d_{540}$
Vertical displacements	$V_{60}, V_{300}, V_{540}$
Pullout force	F

***Pullout test material***

The backfill soils used in this study are poorly graded sub-round gravelly soils, Gravel No.1, Gravel No.3 and Gravel No.5 (Fig. 2). Their particle sizes are 3~5 mm, 7~10 mm and 12~10mm. As shown in Fig. 3, two types of geocell reinforcements were prepared: square-shaped geocell and diamond-shaped geocell. The square-shaped geocell reinforcement was 480 mm (length) × 350 mm (width), having eight square-shape cells in the longitudinal direction and seven square-shape cells in the transverse direction. The longitudinal members have a common height which is 20mm higher than transversal members. Four square-shaped geocell reinforcements with different heights were prepared. The full height (H) of transverse members is 12.5 mm (SG-1); 25 mm (SG-2); 40 mm (SG-3); and 60 mm (SG-4). The diamond-shaped geocell reinforcement was 480 mm (length) × 360 mm (width), having eight diamond-shaped cells in both longitudinal direction and transverse direction. Both types of geocell reinforcements were made of polyethylene terephthalate (PET) covered with PVC for protection, having a thickness of 1 mm. The ultimate tensile strength of the material is 56 kN/m at a strain of 20%. All test cases are summarized in Table 2.

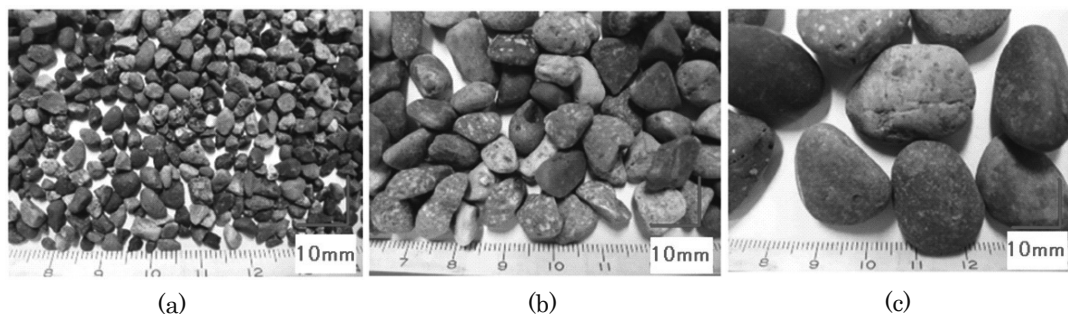


**Figure 2.** Soil materials: (a) Gravel No.1; (b) Gravel No.3; (c) Gravel No.5

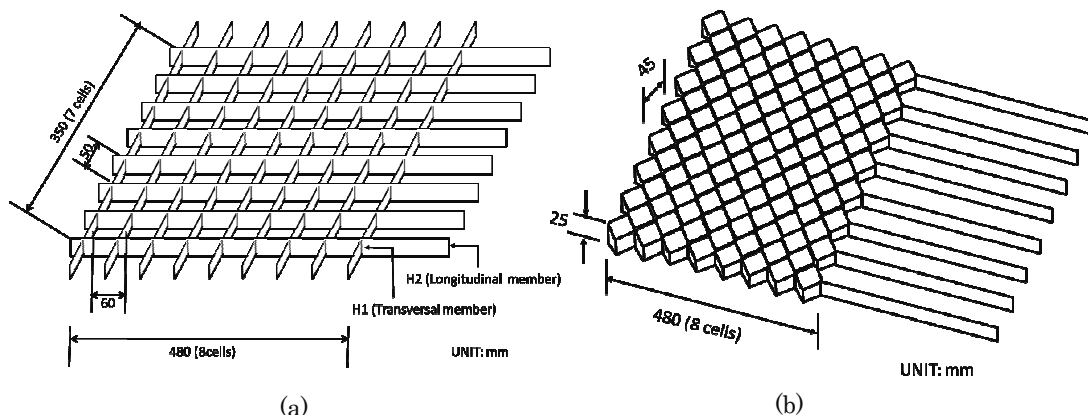


**Figure 4.** Schematic diagram geocell reinforcements: (a) square-shaped geocell reinforcement; (b) diamond-shaped geocell reinforcement

**Table 2** Test cases

Geocell	Height (transversal)	Height (longitudinal)	Backfill material
DG	25 mm	25mm	Gravel No.1
SG-1	12.5 mm	25mm	Gravel No.1
SG-2	25 mm	40mm	Gravel No.1
SG-3	40 mm	60mm	Gravel No.1
SG-2	25 mm	40mm	Gravel No.3
SG-3	40 mm	60mm	Gravel No.3
SG-4	60 mm	80mm	Gravel No.3
SG-3	40 mm	60mm	Gravel No.5
SG-4	60 mm	80mm	Gravel No.5

## RESULTS AND DISCUSSION

### *Effects of geometry of geocell*

Figures 5, 6 and 7 show different pullout characteristics of diamond-shaped geocell and square-shaped geocell. Figure 5 exhibits the relationship between the pullout resistance ( $T$ ) and the horizontal displacement ( $D_{60}$ ) of square-shaped geocell (SG-2) and diamond-shaped geocell (DG), which has the same height (25mm) as SG-2. Square-shaped geocell shows both higher peak resistance and higher initial stiffness than diamond-shaped geocell. Diamond-shaped geocell (DG) starts obvious yielding at very small displacement (2mm) and exhibits strain-hardening, while square-shaped geocell (SG-2) exhibits higher peak strengths at large displacements (16mm), followed by noticeable strain-softening. This difference is due likely to the different geometries of the geocells, in particular the shape of aperture (Fig. 7).

Figures 6 and 7 show the deformation characteristic of diamond-shaped geocell and square-shaped geocell subjected to a pullout force. For diamond-shaped geocell (Figs. 6a and 7a), from  $t_0$  (initial state) to  $t_1$  (the first stage), the first diamond cell starts to deform and provides corresponding pullout resistance (Fig. 5a) until other cells reach the residual resistance state of the first cell. Afterwards from  $t_1$  to  $t_2$ , the second and the third cells deform and provide their pullout resistances until the rest cells reach the residual state of them. This procedure repeats from  $t_2$  to  $t_3$  until all cells work in the pullout process. This deformation characteristic of diamond-shaped geocell can be described as progressive deformation, which induces a lower peak pullout resistance and initial stiffness compared with the

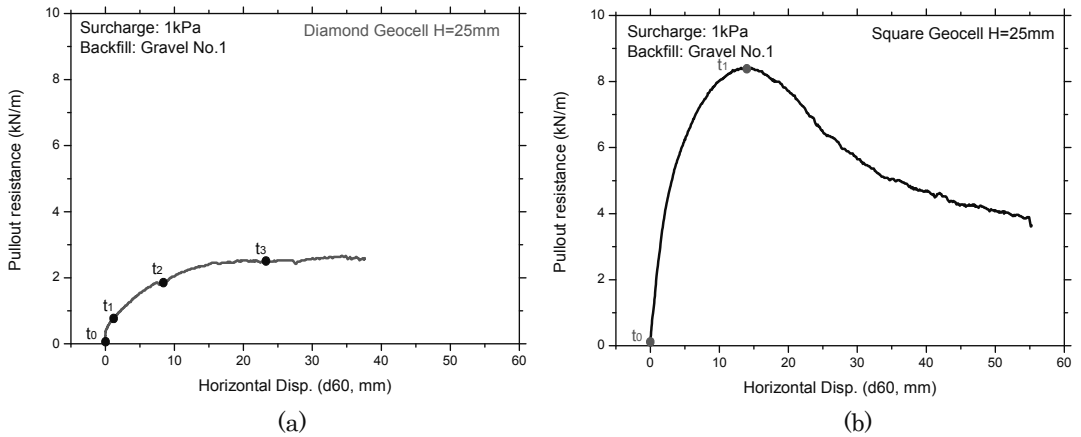


**Figure 5.** Pullout resistance against horizontal displacements ( $d_{60}$ ): (a) diamond-shaped geocell; (b) square-shaped geocell

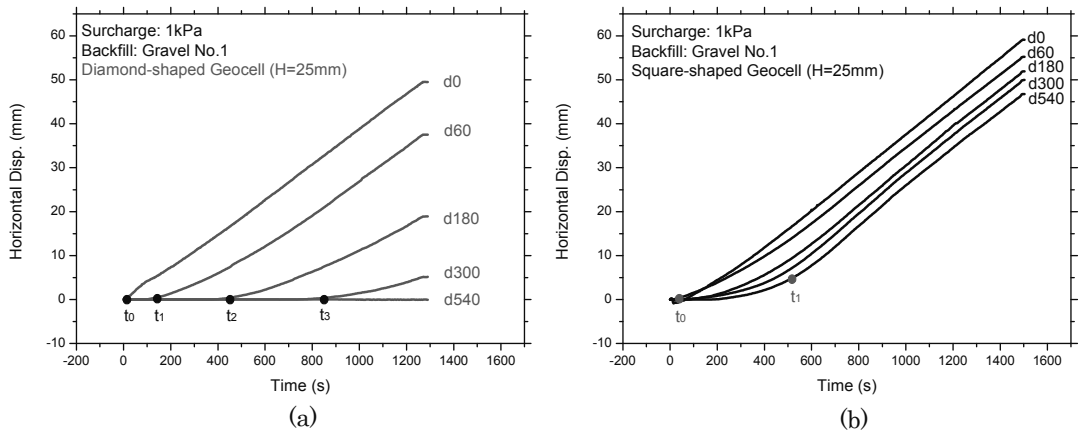


**Figure 6.** Horizontal displacement along the geocell reinforcements versus time history: (a) diamond-shaped geocell; (b) square-shaped geocell

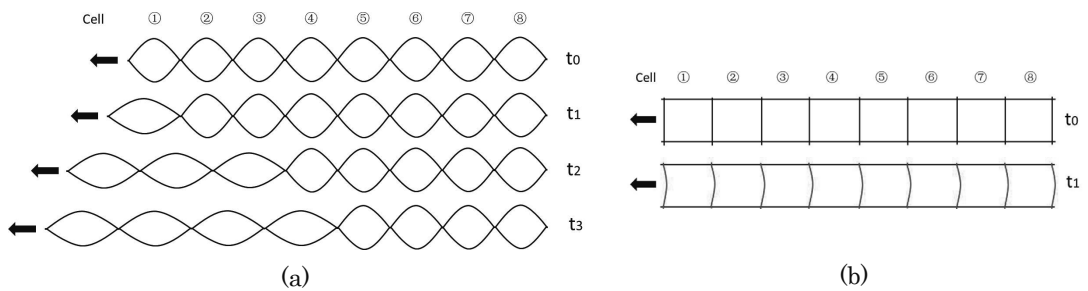
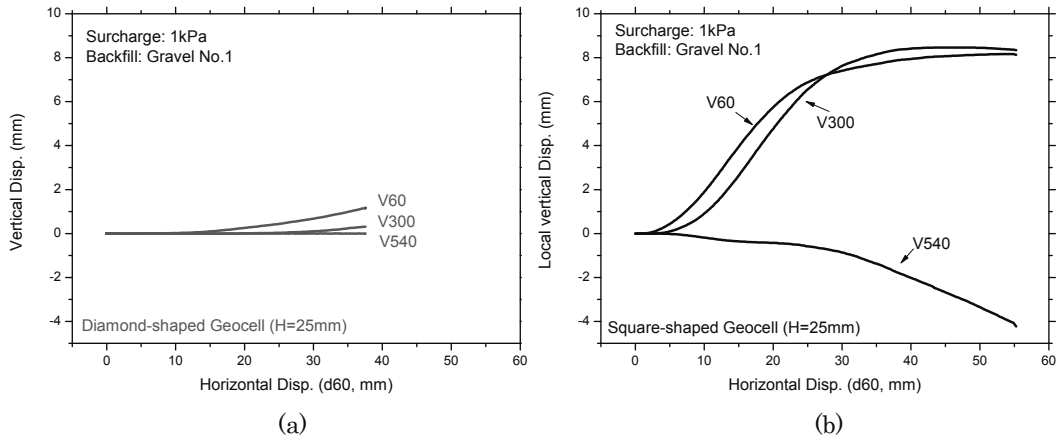


**Figure 7.** Schematic diagram of deformation status vary with time: (a) diamond-shaped geocell and (b) square-shaped geocell

square-shaped geocell. As shown from Fig. 5b, Fig.6b and Fig. 7b, the square-shaped geocell does not

show or show slightly progressive deformation. From  $t_0$  (initial state) to  $t_1$  (peak state), almost all square cells work immediately, which can provide larger peak pullout resistance and higher initial stiffness than diamond-shaped geocell.

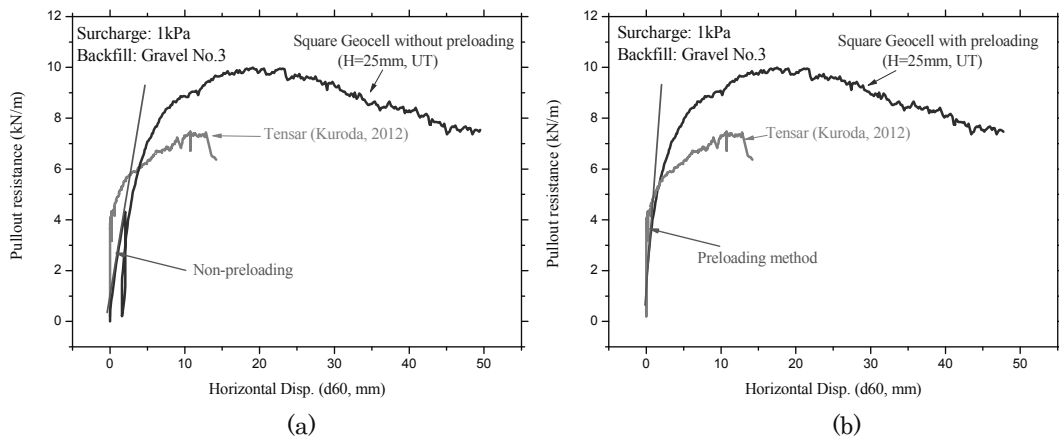
This progressive deformation of diamond-shaped geocell also indicates that the diamond-shaped geocell was not fully mobilized in the soil when subjected to pullout force, which would induce a lower initial stiffness and pullout resistance. This fact can be demonstrated by Figure 8: the soil around diamond-shaped geocell shows slight dilatancy compared with square-shaped geocell under the surcharge of 1kPa.



**Figure 8.** Relationship between horizontal displacement ( $d_{60}$ ) and local vertical displacement ( $V_{60}$ ,  $V_{300}$ ,  $V_{540}$ ): (a) diamond-shaped geocell and (b) square-shaped geocell

### Enhancement of initial stiffness

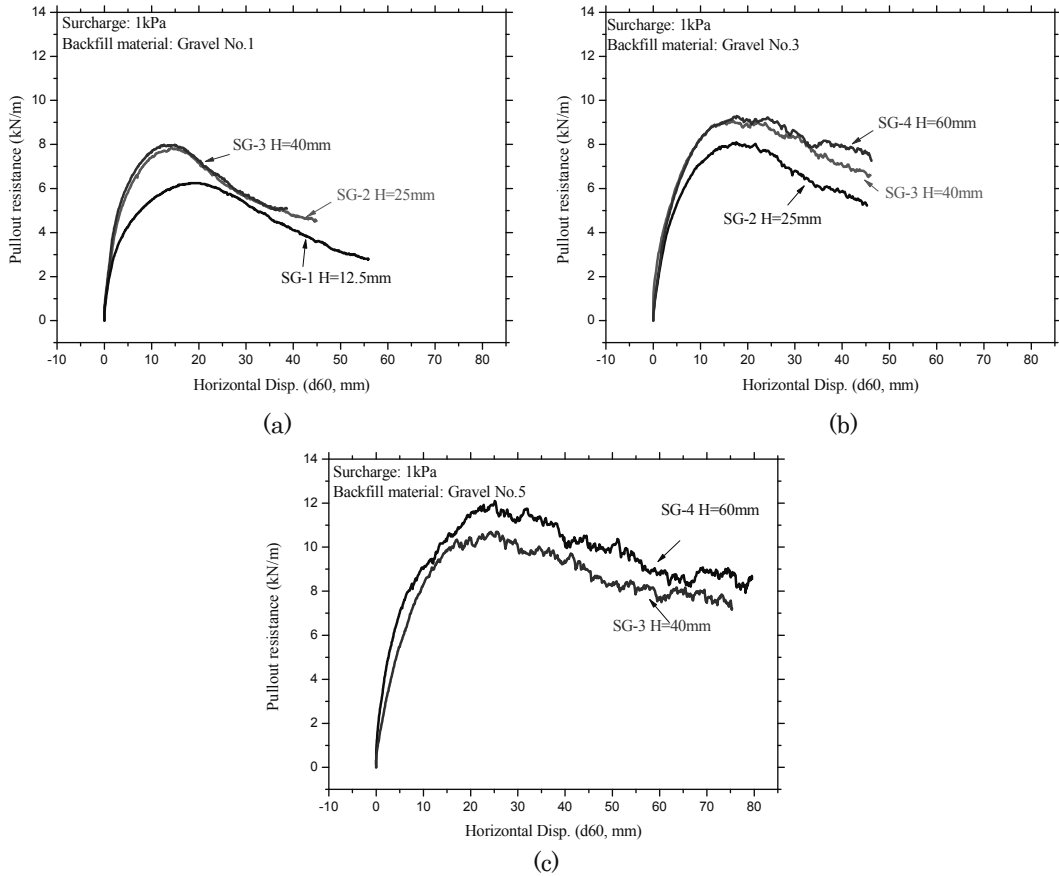
With square-shaped geocells, the initial stiffness increases with an increase in the stiffness of transverse members. Tensar, which are a kind of geogrids and widely used in actual work, has a very high value of this stiffness; therefore it exhibits a very high initial stiffness as seen from Fig. 9. It may also be seen from Fig. 9 that, with geocell SG-1, the initial stiffness increases by applying preloading of pull-out load up to 4.3kN/m. This may be due to that preloading decreased the slackness of the initial arrangement of the transversal members.



**Figure 9.** Relationship between pullout force and horizontal displacement between square-shaped geocell and Tensar: (a) without and (b) with preloading

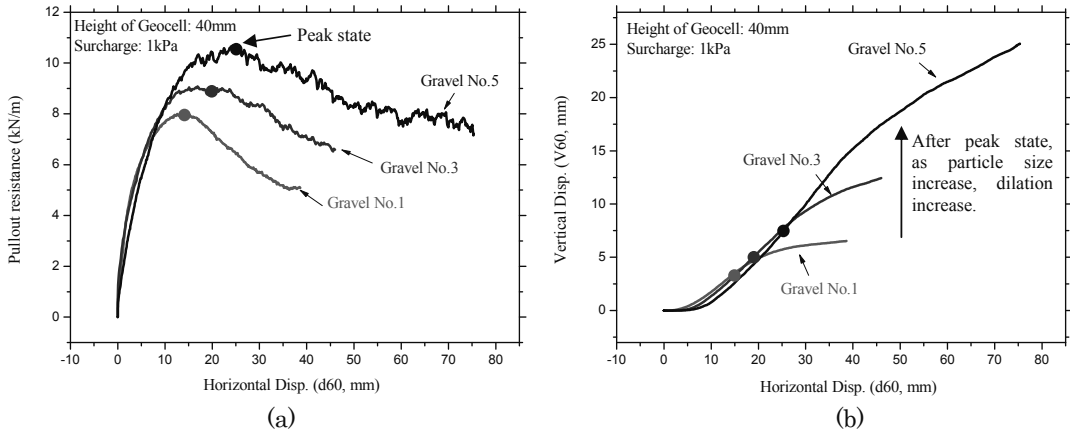
### Effects of particle size relative to aperture size

The relative particle size effect was investigated by using square-shaped geocell with different heights arranged in backfill Gravels No.1 ( $D_{50}=4.5\text{mm}$ ), No. 3 ( $D_{50}=8.5\text{mm}$ ) and No. 5 ( $D_{50}=16\text{mm}$ ). It may be seen from Fig. 10 that, with an increase in the particle size, the peak strength increases while the amount strain softening decreases: i.e., the residual strength increases with an increase in the particle size to a more extent than the peak strength.



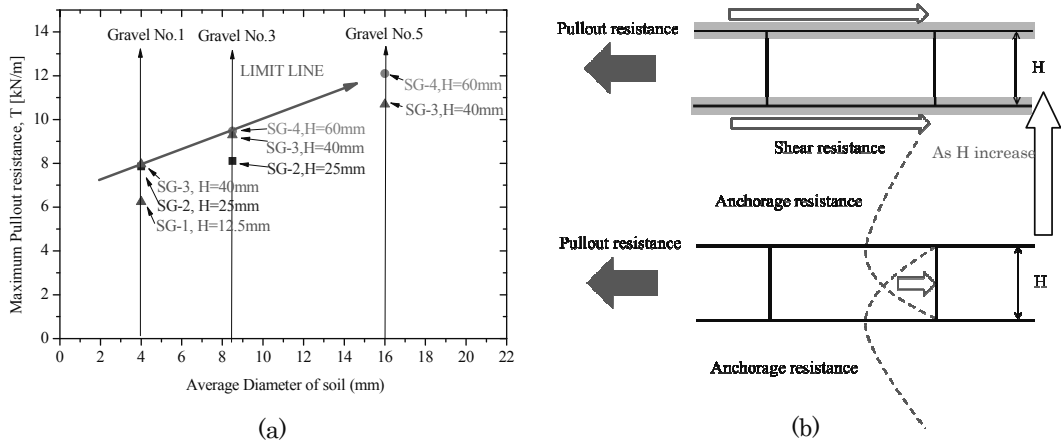
**Figure 10.** Pullout behavior of square-type geocells with different heights: (a) Gravel No.1; (b) Gravel No.3; (c) Gravel No.5

Figure 11 compares the effects of backfill particle size on the pull-out resistance and the local vertical displacements ( $V_{60}$ ) measured above the geocell SG-3 (shown in Figure 1) plotted against the pullout displacement ( $D_{60}$ ). In the post-peak regime, the rate of dilatancy per horizontal displacement was larger while the strain-softening was smaller with Gravel No.5 (larger particles) than with Gravel No.3 and No.1 (smaller particles). This result indicates that, with an increase in the backfill particle size, the shear band that develops at the interfaces between the geocell and the backfill becomes thicker, therefore the ultimate amount of dilatancy becomes larger, which results in a larger increases in the local vertical stress activated to the geocell, therefore larger pull-out resistance at large pull-out displacements.



**Figure 11.** Relationship between horizontal displacement and pullout resistance, local vertical displacement ( $V_{60}$ ) of SG-3 ( $H=40\text{mm}$ )

The pull-out resistance increases with an increase in the member height from 12.5 mm to 25 mm in Figure 10a, from 25 mm to 40 mm in Figure 10b and from 40 mm to 60 mm. However, with further increase in the member height, the pull-out resistance exhibits only a very small increase in Gravel No.1 and No.3 cases. To analyze this trend, Figure 11a summarizes the pull-out resistance of square-shaped geocells SG-1, SG-2, SG-3 & SG-4 embedded in Gravel No.1, Gravel No.3 and Gravel No.5. It may be seen that, under otherwise the same conditions, the pull-out resistance increases with an increase in the member height with the square-shaped geocells. However, there exists an upper limit with the pullout resistance that is reached when the height of member or member becomes a certain value that increases with an increase in the backfill particle diameter. The line presented in Figure 12a indicates this upper-limit state.



**Figure 12.** (a) Particle size effect on maximum pullout resistance; and (b) two mechanism of pullout resistance of reinforcement embedded in the backfill

These test results suggest the following fundamental mechanism. As shown in Figure 12b, the pullout resistance is equal to the smaller one of the following two types of resistance: 1) the shear resistance of the shear bands that develop along the upper and bottom faces of a geocell and the backfill, which is independent of the height of member or member (i.e., the height of geocell); and 2) the anchorage resistance induced by passive pressure developing inside the cells, which increases with an increase in the height of geocell. Therefore, as the height of geocell increases, the total pullout



resistance is first determined by the anchorage resistance and increases with an increase in the height of geocell. When the height of geocell reaches a certain value, the anchorage resistance reaches the shear resistance. Then, the pull-out resistance does not increase with further increase in the height of geocell. Both shear resistance and anchorage resistance increase with an increase in the backfill particle size, therefore the pull-out resistance does so. This trend becomes stronger at larger pull-out displacements. The test results show that the limit of the height of geocell at which the two types resistance become the same increase in the backfill particle size.

## CONCLUSIONS

A geocell having square-shaped apertures was developed to increase the pull-out resistance. A series of pullout tests were conducted on small scaled models of square-shaped geocell as well as diamond-shaped geocell arranged in backfill of gravelly soil. By analyzing the data from these tests, the effects of the shape of cell and the height of transversal members (ribs) and the backfill particle size on pullout resistance were evaluated. The main conclusions from this study are as follows:

1. The effects of cell shape increases with an increase in the pull-out displacement. Under otherwise the same conditions, two types of geocell show different pullout characteristics: the progressive deformation characteristic of diamond-shaped geocell and non-progressive deformation characteristic of square-shaped geocell. Due to this effect, the square-shaped geocell exhibits much higher peak pull-out resistance and higher initial stiffness than the diamond-shaped geocell.
2. The initial pull-out stiffness of a geocell increases by reducing the initial slackness of the geocell by preloading.
3. The pullout resistance is equal to the smaller value of: 1) the shear resistance of the shear bands along the upper and bottom faces of a geocell, which is independent of the height of geocell; and 2) the anchorage resistance induced by passive pressure developing inside the cells, which increases with an increase in the height of geocell. Therefore, as the height of geocell increases, the total pullout resistance is equal to the anchorage resistance and increases with an increase in the height of geocell. When the height of geocell reaches a certain value, the pull-out resistance becomes the same as the shear resistance and does not increase with further increase in the height of geocell. Both shear resistance and anchorage resistance, therefore the pull-out resistance, increase with an increase in the backfill particle size.

The tests results presented in this paper are rather limited, for example, the limit value for Gravel No.5 was not reached due to the limitation of height of geocell. More tests to evaluate the effects of the stiffness and height of geocell and the particle diameter of backfill, the vertical pressure and so on should be tested in the future.

In addition, the pullout behavior of different types of geocells may be different under larger surcharge, since other factors, for instance, the connection between cells, may govern the ultimate pullout resistance. Therefore, the tests should also be conducted under larger surcharge in the future.

## ACKNOWLEDGEMENTS

The author sincerely appreciates the help of Mr. Michiyuki HARATA in TOKYO PRINTING INK MFG. CO., LTD to provide the geocell models, which can make the experiments proceeds smoothly.

## REFERENCES

- Dash, S.K., Krishnaswamy, N.R., and Rajagopal, K. (2001a). "Bearing capacity of strip footings supported on geocell-reinforced sand." *Geotextiles and Geomembranes*, 19(4), 235-256.
- Dash, S.K., Rajagopal, K., and Krishnaswamy, N.R. (2001b). "Strip footing on geocell reinforced sand beds with additional planar reinforcement." *Geotextiles and Geomembranes*, 19(8), 529-538.
- Dash, S.K., Rajagopal, K. and Krishnaswamy, N.R. (2004). "Performance of different geosynthetic

- reinforcement materials in sand foundations.” *Geosynthetics International*, 11(1), 35-42.
- Dash, S.K., Sireesh, S., and Sitharam, T.G. (2003). “Model studies on circular footing supported on geocell reinforced sand underlain by soft clay.” *Geotextiles and Geomembranes*, 21(4), 197-219.
- Kiyota, T., Soma, R., Munoz, H., Kuroda, T., Ohta, J., Harata, M., and Tatsuoka, F. (2009). “Pullout behaviour of geo-cell placed as reinforcement in backfill.” *Geosynthetics Engineering Journal* 24(0), 75-82. (In Japanese).
- Kuroda, T., (2012). “Evaluation of static and seismic stability of bridges with reinforced backfill and integrated structural (New type and Rehabilitated type bridges) by model tests.” *Master thesis, Department of civil engineering, Tokyo University of Science.* (In Japanese).
- Ling, H.I., Leshchinsky, D., Wang, J.P., Mohri, and Y., Rosen, A. (2009). Seismic response of geocell retaining walls: experimental studies. *ASCE Journal of Geotechnical and Geoenvironmental engineering* 135, 515-524.
- Mhaiskar, S.Y. and Mandal, J.N. (1992). “Comparison of a geocell and horizontal inclusion for paved road structure.” *Proceedings of the International Symposium on Earth Reinforcement Practice*, 1, 641.
- Mhaiskar, S.Y. and Mandal, J.N. (1994). “Three dimensional geocell structure: performance under repetitive loads”, *5th International Conference on Geotextile, Geomembranes and Related products, Singapore*, 155-158.
- Rea, C. and Mitchell, K. (1978). “Sand reinforcement using paper grid cells.” *Proceedings, Symposium on Earth Reinforcement, ASCE Annual Convention, Pittsburgh, PA*, 644-663.
- Shimizu, M. and Inui, T. (1990). “Increasing in the bearing capacity of ground with geotextile wall frame.” *Geotextiles, Geomembranes and Related Products*, 254.
- Tatsuoka, F., Koseki, J., and Tateyama, M. (2009). “Seismic behaviour of geosynthetic-reinforced structures: Lessons from recent earthquakes and from recent earthquakes and design approaches.” *The 12th Italian Conference on Geosynthetics, Italy*.
- Yuu, J., Han, J., Rosen, A., Parson, R., Leshchinsky, D. (2008). Technical review of geocell-reinforced base courses over weak subgrade. *International Proceeding of First Pan American Geosynthetics Conference and Exhibition, Cancun, Mexico*: 1022-1030.